Phonons in cesium

N. Nücker
Kernforschungszentrum Karlsruhe, Institut für Nukleare Festkörperphysik, P. O. B. 3640, D-7500 Karlsruhe, Federal Republic of Germany

U. Buchenau
Institut für Festkörperforschung der Kernforschungsanlage Jülich, P. O. B. 1913, D-5170 Jülich, Federal Republic of Germany

(Received 22 October 1984)

Inelastic neutron time-of-flight spectra from polycrystalline cesium were measured at 50, 100, and 290 K for a large variety of momentum transfers Q and energy transfers ω. Born–von Kármán models were fitted to the resulting (Q,ω) topography. These models were used to calculate the phonon dispersion curves and the phonon densities of states. The results confirm theoretical predictions. The elastic constants c_{44} and c' determined from the measured data agree with ultrasonic results.

INTRODUCTION

In this paper we report on inelastic neutron scattering experiments on cesium. So far the only information about the lattice dynamics of cesium consists of the elastic constants measured by the ultrasonic-pulse-echo technique[1] and specific heat measurements.[2–4] Theoretical investigations on the basis of various models have been done to predict dispersion relations,[5–9] the phonon density of states,[9,10] the heat capacity,[11] and pressure-dependent phenomena.[12–14]

Inelastic neutron scattering experiments on cesium pose some experimental problems due to its chemical reactivity and the large neutron absorption cross section ($\sigma_a = 29b$ at 25 meV) compared to a fairly low coherent scattering ($\sigma_c = 3b$). The phonon spectrum of cesium ends at about 1 THz, much lower than the phonon frequencies of any useful sample-container material.

In a classical phonon scattering experiment the dispersion curves are measured by inelastic neutron scattering from a single crystal using a triple-axis spectrometer. Another approach was described and tested by Buchenau.[15,16] In this method inelastic neutron scattering from polycrystalline samples is measured in a wide range of momentum transfer Q and energy transfer $\hbar\omega$. Owing to the momentum selection rule $\mathbf{Q}=\mathbf{G}+\mathbf{q}$ ($\mathbf{G}$ is a reciprocal lattice point, $\mathbf{q}$ is a phonon wave vector) the coherent one-phonon scattering process introduces Q-dependent structures for constant energy transfers. The resulting (Q,ω) topography incorporates a lot of information on the lattice dynamics which can be extracted by fitting lattice dynamical models, e.g., Born–von Kármán or pseudopotential models, to it. Time-of-flight instruments are most suitable for this method, as all the topography is measured at once and hence only short measuring times are needed.

EXPERIMENT

20 g of cesium of nominal purity 99.98% was placed into a quartz ampoule with 16.8 mm inner diameter and sealed.

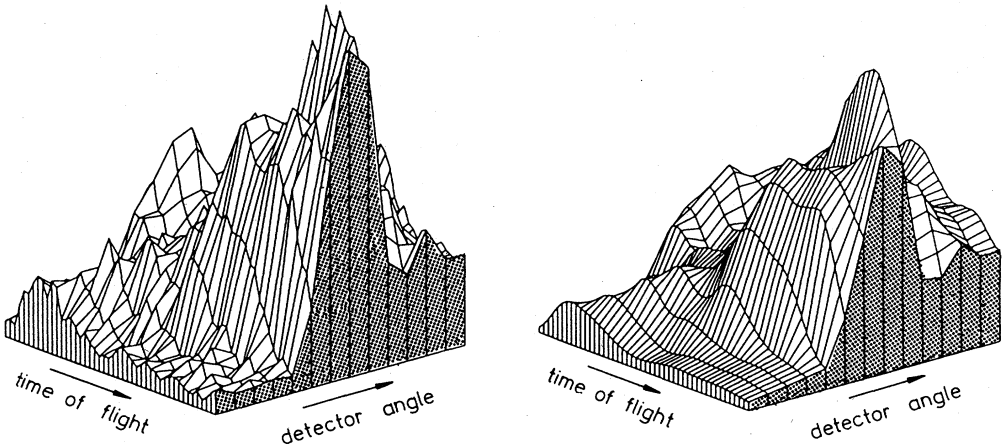

FIG. 1. (a) Neutron time-of-flight spectra of cesium at 100 K corrected for sample container, self-absorption multiple and multiphonon scattering, and detector efficiency. (b) Computed time-of-flight spectra using fitted Born–von Kármán parameters.

TABLE I. Elastic constants of cesium in GPa.

	This study			Kollarits *et al.* (Ref. 1)	
	50	100	290	4	78
		(K)		(K)	
c_{44}	1.0 ± 0.3	1.0 ± 0.3	1.2 ± 0.3	1.60 ± 0.06	1.48 ± 0.06
$c' = \frac{1}{2}(c_{11} - c_{12})$	0.19 ± 0.05	0.17 ± 0.03	0.10 ± 0.03		0.20 ± 0.03
$c_n = \frac{1}{2}(c_{11} + c_{12} + 2c_{44})$				3.98 ± 0.16	3.74 ± 0.15

Precautions were taken to ensure that the cesium sample had no preferential orientation: The sample was liquified and then immersed into acetone cooled to about 240 K. The sample was stirred by shaking the ampoule during solidification. After this treatment the sample was transferred to the cryostat and cooled down to 50 K. To suppress the influence of any remaining sample orientation the sample was rotated at about 100 rpm during the measurement.

The IN6 time-of-flight spectrometer on a cold-neutron guide beam of the Institute Laue-Langevin (ILL) reactor was chosen for this experiment because of its intense neutron flux and good resolution at low energies. The energy of the incoming neutrons was set to $E_0 = 3.085$ meV. The range of the 337 elliptical ^{3}He detectors was 10.7° to 114.3°, covering a Q range 0.23 $\text{Å}^{-1} \leq Q \leq 2.07$ Å^{-1}. The spectrometer resolution was optimized for elastic scattering by rotating the chopper at 6061 rpm. At this chopper speed the neutrons from the three subsequent graphite monochromators are focused in time at the counters. Since the energy transfer of interest in the cesium experiment is very low (0–4.5 meV), the energy spread in E_0 of the three graphite monochromators has only a minor effect on the resolution.

All measurements were performed in energy gain scattering. For intensity reasons the lowest sample temperature was 50 K. Further measurements were done at 100 and 290 K. Empty container measurements were performed at the same temperatures. For intensity calibration a vanadium sample was measured.

RESULTS AND DISCUSSION

Figure 1 shows the measured neutron time-of-flight topography of cesium at 100 K. The measured intensities were already corrected for the scattering of the quartz container, for self-absorption, multiple, and multiphonon scattering and for detector efficiency. Born–von Kármán parameters were fitted to these data. Force constants up to the third neighbor gave satisfactory fits. The number of free parameters in these fits was reduced to four by including the elastic constants (Table I) into the calculations. The distribution calculated with the fitted Born–von Kármán constants is compared with the measured distribution in Fig. 1. The Born–von Kármán parameters for 50, 100, and 290 K are listed in Table II. Figure 2 shows the resulting dispersion curves both for 290 and 50 K.

TABLE II. Born–von Kármán constants of cesium.

Neighbor and indices	Force constants (dyn/cm)		
	$T = 50$ K	$T = 100$ K	$T = 290$ K
1 *XX*	506.4	533.2	556.1
1 *XY*	599.6	610.6	557.8
2 *XX*	347.5	350.7	334.4
2 *XY*	−15.3	−23.2	−84.8
3 *XX*	−27.1	−34.6	−57.5
3 *ZZ*	5.4	3.4	−11.8
3 *XY*	32.5	−38.0	−45.8

When we compare our results with theoretical predictions (Table III) we observe in general good agreement. The harmonic calculation using a first principles pseudopotential[5] gives rather high values for the longitudinal phonons at N, at P, and at $\eta = (0.35, 0.35, 0.35)$ compared with the other theoretical predictions[6–9] and to our results. Comparing the results at 0 K of Ref. 5 with those at 290 K of Ref. 6, including cubic terms in the pseudopotential calculations, a phonon softening upon heating is predicted for all frequencies. Our results show the same trend except in the vicinity of the H point of the reciprocal lattice. This discrepancy may be due to experimental difficulties encountered mainly at the upper end of the frequency spectra.

The phonon softening is also reflected in the phonon density of states (Fig. 3) calculated from the Born–von Kármán models. For comparison we included the predicted phonon density of states by Vaks *et al.*[10] into Fig. 3. Both distributions are similar in shape but the predicted phonon density of states[10] is shifted to higher frequencies.

Specific-heat measurements[2–4] may be compared with our

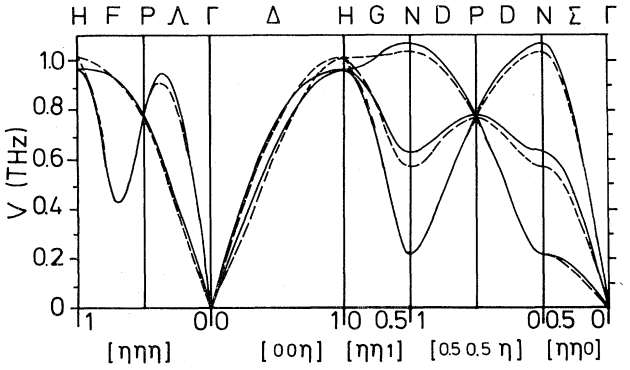

FIG. 2. Dispersion relation of cesium ($T = 50$ K, ——; $T = 290$ K, – – –).

TABLE III. Comparison of measured and predicted phonon frequencies (THz). (H = harmonic; QH = quasiharmonic; SCH + C = self-consistent harmonic + cubic term; OMP = optimized model potential; MOMP = modified energy-dependent model pseudopotential; HPAM = homology of phonons in the alkali metals; AFM = angular force model).

	Mode		H 15	N 4′	N 3′	N 1′	Λ_1 ($\eta=0.35$)	P 4	F_1 at. 7
	This result	$T=50$ K	0.96	0.22	0.63	1.07	0.97	0.78	0.49
		$T=100$ K	0.99	0.23	0.64	1.08	0.96	0.79	0.44
		$T=290$ K	1.01	0.22	0.57	1.04	0.91	0.77	0.42
		Error[a]	0.05	0.01	0.03	0.05	0.05	0.04	0.02
(5)	H	$T=0$ K	1.02	0.24	0.66	1.19	1.05	0.90	0.44
(6)	QH	$T=290$ K	0.95	0.21	0.62	1.07	0.97	0.82	0.41
	SCH + C		0.91	0.25	0.57	1.07	0.95	0.81	0.40
(7)	OMP		1.05	0.22	0.74	1.09	0.99		0.49
	MOMP		1.05	0.22	0.74	1.05	0.96		0.48
(8)	HPAM		0.94	0.27	0.66	1.05	0.95	0.79	0.46
(9)	AFM		0.94	0.22	0.66	1.05	0.94	0.77	

[a]The frequency error was estimated to be about 5% including corrections for self-absorption and multiphonon scattering as well as the influence of statistics and the least-squares procedure.

results with the help of the temperature-dependent Debye temperature $\theta(T)$ (Fig. 4). Our results are up to 5% (Ref. 2) respective 8% (Ref. 3) lower than the specific-heat result.

The intensity variation of the low-energy transfer data (energy transfer range: 0.066 to 0.164 THz) in the Q range of the (110) and (002) Bragg reflections ($G_{110}=1.475$ Å^{-1}, $G_{002}=2.086$ Å^{-1}) was used to determine the elastic constants. At sufficiently low energy transfers the intensity of scattered neutrons near Debye-Scherrer rings (shaded area in Fig. 1) is related to the sound velocities and hence to the elastic constants:[17]

$$J(Q,\omega)\sim k_B T\int dq \sum_{n=1}^{3}(\mathbf{G}\mathbf{e}_{qn})^2/c_n^2$$

($\mathbf{e}_{qn}$ is an eigenvector of the phonon mode n with wave vector $\mathbf{q}$ and velocity c_n). Figure 5 shows the measured intensities together with a least-squares fit for the elastic constants (full line). The resulting elastic constants are compared with ultrasonic pulse echo technique results by Kollaritis and Trivisonno[1] in Table I. The two techniques are com-

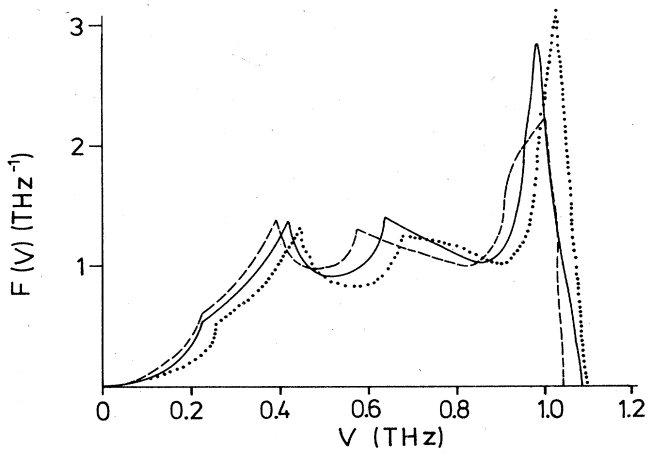

FIG. 3. Phonon density of states [50 and 100 K, ——; 290 K, — — —; predictions by Vaks *et al.* (Ref. 10), · · · ·].

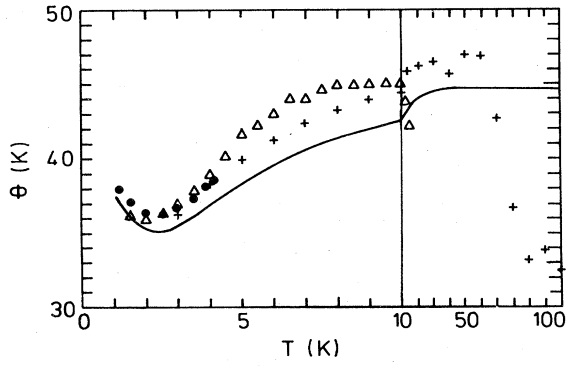

FIG. 4. Debye temperature of cesium (50 and 100 K, ——; Ref. 2, +; Ref. 3, ●; Ref. 4, Δ).

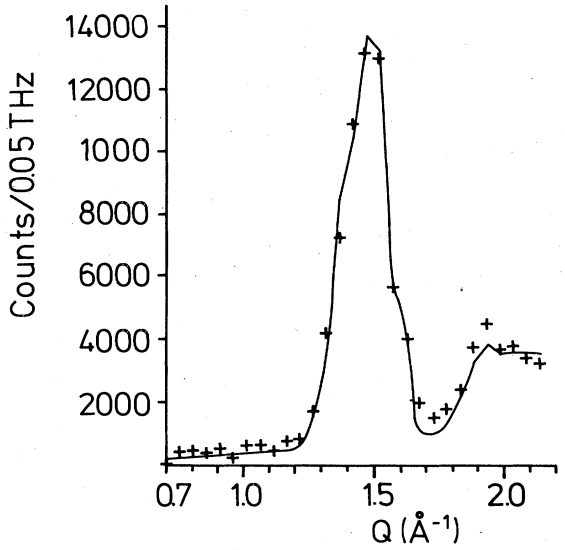

FIG. 5. Fit of elastic constants (——) to measured intensities (+) at low phonon energies. ($T = 100$ K, energy range 0.11–0.16 THz).

plementary, because the small c' is better determined in the neutron measurement, while this method is fairly insensitive to the two large elastic constants c_{11} and c_{44}.

CONCLUSIONS

In this paper we showed that inelastic neutron scattering on polycrystalline cesium is an adequate method for determining the lattice dynamics of cesium. While single-crystal measurements on zero-pressure cesium would be of interest for investigating the linewidth of phonons, our method seems most promising to explore the lattice dynamics of cesium under pressure. The phonon dispersion curves are in good agreement with most theoretical predictions.

ACKNOWLEDGMENTS

We would like to express our thanks to W. Reichardt and W. Weber for helpful discussions. We thank the staff of Institute Laue-Langevin for support during the experiment.

[1]F. J. Kollarits and J. Trivisonno, J. Phys. Chem. Solids **29**, 2133 (1968).
[2]J. D. Filby and D. L. Martin, Proc. R. Soc. London Ser. A **284**, 83 (1965).
[3]W. H. Lien and N. E. Phillips, Phys. Rev. A **133**, 1370 (1964).
[4]D. C. McCollum, Jr. and H. B. Silsbee, Phys. Rev. **127**, 119 (1962).
[5]R. Taylor and A. H. MacDonald, J. Phys. F **10**, 2387 (1980).
[6]H. R. Glyde and R. Taylor, Phys. Rev. B **25**, 6500 (1982).
[7]C. B. So and S. Wang, J. Phys. F **7**, 35 (1977).
[8]V. Ramamurthy and M. Satishkumar, Physica B **111**, 297 (1981).
[9]S. Jogi, J. Phys. F **4**, 11 (1974).
[10]V. G. Vaks, N. E. Zein, S. P. Kravchuk, and A. V. Trefilov, Phys. Status Solidi B **96**, 857 (1979).
[11]V. G. Vaks, E. V. Zarochentsev, S. P. Kravchuk, V. P. Safronov, and A. V. Trefilov, Phys. Status Solidi B **85**, 63 (1978).
[12]R. Srinivasan and K. S. Girirajan, J. Phys. Chem. Solids **34**, 611 (1973).
[13]D. Glötzel and A. K. McMahan, Phys. Rev. B **20**, 3210 (1979).
[14]T. Soma and E. Ueda, J. Phys. F **12**, 59 (1982).
[15]U. Buchenau, H. R. Schober, J.-M. Welter, G. Arnold, and R. Wagner, Phys. Rev. B **27**, 955 (1983).
[16]U. Buchenau, M. Heiroth, H. R. Schober, J. Evers, and G. Oehlinger, Phys. Rev. B **30**, 3502 (1984).
[17]U. Buchenau, Solid State Commun. **32**, 1329 (1979).